CrystEngComm

PAPER

View Article Online
View Journal | View Issue

Cite this: *CrystEngComm*, 2014, **16**, 9308

Evaluation of structural transformation in 2D metal–organic frameworks based on a 4,4′-sulfonyldibenzoate linker: microwave-assisted solvothermal synthesis, characterization and applications†

Cheng-You Wu,[a] Duraisamy Senthil Raja,[b] Chun-Chuen Yang,*[c] Chun-Ting Yeh,[a] Yu-Ru Chen,[a] Chen-Yu Li,[a] Bao-Tsan Ko*[d] and Chia-Her Lin*[a]

Received 11th June 2014,
Accepted 18th August 2014

DOI: 10.1039/c4ce01201a

www.rsc.org/crystengcomm

Six 2D metal–organic frameworks containing V-shaped 4,4′-sulfonyldibenzoate (SBA) linkers, $[Zn_3(SBA)_2(OH)_2]\cdot EtOH$ (**1** or **CYCU-5**·EtOH), $[M_3(OH)_2(SBA)_2(EtOH)(H_2O)_3]\cdot 3.5H_2O$ (**2**–**4**, M = Mg, Ni, and Co), [Mn(SBA)(EtOH)] (**5**) and $[Mn(SBA)(H_2O)]$ (**6**), have been synthesized rapidly under microwave-assisted solvothermal conditions. The structural analysis revealed that all compounds display two-dimensional structures containing inorganic motifs with one-dimensional chains (**1**–**5**) or dimers of trigonal prisms (**6**) connected through SBA linkers and forming 2D neutral and porous channels. Compounds **1**–**4** were further characterized by elemental analysis, thermogravimetric analysis (TGA), powder X-ray diffraction (PXRD) measurements and IR spectroscopy. The desolvated phases of compounds **1**–**2**/**3**–**4** have thermal stabilities up to about 400/350 °C. The desolvated frameworks of **1**–**4** above 200 °C have similar **CYCU-5**-like conformations and exhibit gas adsorption properties with N_2, CO_2 and H_2 gases. Interestingly, **CYCU-5** displays selective adsorption of CO_2 over N_2 and CH_4 gases at 273 K. In addition, the catalytic ability of **CYCU-5** as an initiator for ring-opening polymerization of L-lactide has also been demonstrated.

Introduction

Metal–organic frameworks (MOFs) have been intensively studied in recent years because of their fascinating structural diversities and topologies as platforms for various functional applications.[1,2] They are built up of metal ions interconnected by organic linkers, thus mostly forming two- or three-dimensional porous frameworks. In order to achieve a diverse range of structures, various routes such as room temperature synthesis, conventional electronic heating, microwave heating, electrochemistry, mechanochemistry, and ultrasonic methods have been employed.[3] Particular attention has been paid to microwave-assisted solvothermal reactions, mainly because of their greener approach to synthesize materials in a shorter reaction time and with less power consumption than that of conventional solvothermal synthetic methods.[4]

It is obvious that the design of MOF materials depends on careful choice of the building blocks such as metal ions, organic linkers, co-ligands, and adequate solvents, and their proper organization in the solid state.[5] Among them, the selection of organic linkers is one of the significant aspects.[6] This is because the configurations, rigidities, substituents and coordination modes of organic ligands have played vital roles in determining the structural properties of the MOFs. In this context, V-shaped dicarboxylates as linkers for the construction of MOFs have been in the limelight very recently. In particular, 4,4′-sulfonyldibenzoic acid (H_2SBA) is a typical example of a V-shaped dicarboxylate linker for the construction of novel MOFs as it has six potential donor atoms that allow the formation of variable structural topologies.[7] In this regard, we have recently found and published the fact that V-shaped dicarboxylate ligands such as 4,4′-sulfonyldiebenzoate (SBA) and 4,4′-oxybisbenzoate can be used to construct a variety of MOFs with robust structures.[8]

[a] *Department of Chemistry, Chung Yuan Christian University, Chungli, Taoyuan 320, Taiwan. E-mail: chiaher@cycu.edu.tw; Fax: +886 3 2653399; Tel: +886 3 2653315*
[b] *Department of Chemistry, National Tsing Hua University, Hsinchu 300, Taiwan*
[c] *Department of Physics, Chung Yuan Christian University, Chungli, Taoyuan 320, Taiwan. E-mail: chunchuenyang@cycu.edu.tw*
[d] *Department of Chemistry, National Chung Hsing University, Taichung, 402, Taiwan. E-mail: btko@dragon.nchu.edu.tw*

† Electronic supplementary information (ESI) available: the ESI file contains TGA curves and data of **1**–**4**, PXRD patterns at varied temperatures for **1**–**4**, Rietveld profile fits, the high pressure gas adsorption isotherms and tables showing selected bond lengths and H-bond lengths. CCDC 943771, 943772, 805748, 998723 and 998724. For ESI and crystallographic data in CIF or other electronic format see DOI: 10.1039/c4ce01201a

On the other hand, among the MOFs the 3D frameworks with open channels have largely been known in the recent past, but relatively few examples of 2D open frameworks are found in the literature.[9] Further, the 2D MOFs have been less well known for their gas sorption properties, mainly due to the small interlayer spacings between the 2D layers, which may not be wide enough for the incorporation of gas molecules.[10] Also, the selective adsorption of CO_2 using MOFs[11] has attracted attention in recent years because CO_2 is believed to be the major greenhouse gas that causes global warming.[12]

With this above background in mind, and as a continuation of our research on H_2SBA, herein we report six 2D MOFs, $[Zn_3(SBA)_2(OH)_2]\cdot EtOH$ (**1** or **CYCU-5**·EtOH), $[M_3(OH)_2(SBA)_2(EtOH)(H_2O)_3]\cdot 3.5H_2O$ (**2–4**, M = Mg, Ni, and Co), [Mn(SBA)(EtOH)] (**5**) and [Mn(SBA)(H_2O)] (**6**), which are synthesized under microwave-assisted solvothermal conditions. It is to be noted that the structural description of compound **4** has already been reported,[13] but there is no report on its porous properties. Hence, we report its gas sorption properties along with the other three new compounds (**1**, **2** and **3**). Further, we report only the single crystal X-ray diffraction structural descriptions for compounds **5** and **6** because the yield of both was too low (only very few single crystals have been obtained) for other studies.

Experimental section

Materials and general methods

Chemicals of reagent grade or better were used as received. Microwave-assisted reactions were done in a 100 mL Teflon autoclave placed in a microwave oven (START D, Milestone, maximum power of 1200 W, 2.45 GHz) in which the precursor mixtures were heated for several minutes. All products' phase purity was examined by powder X-ray diffraction (PXRD) before further characterization. Elemental analyses were carried out to confirm the composition of the organic part of the prepared samples. Thermogravimetric analyses (TGA), using a DuPont TA Q50 analyzer, were performed on powder samples under flowing N_2 with a heating rate of 10 °C min^{-1}. FT-IR spectra were recorded in the range of 400–4000 cm^{-1} on a JASCO FT-IR-460 spectrophotometer using KBr pellets. The gas sorption isotherms have been measured at 77 K for N_2 and H_2, and for CO_2 at 273 and 298 K by using a Micromeritics ASAP 2020 adsorption apparatus. About 100 mg of adsorbent was used for the gas sorption studies. The high pressure gas sorption studies were measured on a Quantachrome iSorpHP adsorption system with about 500 mg of each sample. The initial gas removal process was performed under vacuum at 423 K for 12 h. The free space of the system was determined by using He gas. Ultrahigh purity CO_2, N_2, CH_4, H_2 and He gases were used as received in all the gas sorption experiments. Ring-opening polymerization (ROP) of L-lactide (L-LA) catalyzed by **CYCU-5** was carried out by following our previous study.[14]

Synthesis of MOFs

Microwave synthesis of $[Zn_3(OH)_2(SBA)_2]\cdot EtOH$ (1). The compound **1** was obtained from a reaction mixture of H_2SBA (0.1224 g, 0.4 mmol), $Zn(NO_3)_2\cdot 6H_2O$ (0.2360 g, 0.8 mmol), EtOH (9.0 mL) and H_2O (1.0 mL). The mixture was heated at 180 °C for 40 min. The colorless crystals of **1** were filtered off, washed with EtOH, dried at room temperature, and collected with the yield of 0.0782 g (88.41%, based on the H_2SBA reagent). Anal. found/calcd.: C, 40.6/40.9; H, 2.5/2.7% for **1**. IR (KBr, cm^{-1}): 3508(m), 3045(w), 2969(w), 1957(w), 1609(s), 1564(m), 1395(s), 1297(m), 1163(m), 1011(w), 838(w), 784(w), 731(s), 619(m), 432(w).

Microwave synthesis of $[Mg_3(OH)_2(SBA)_2(EtOH)(H_2O)_3]\cdot 3.5H_2O$ (2). A mixture of H_2SBA (0.1224 g, 0.4 mmol), $Mg(NO_3)_2\cdot 6H_2O$ (0.4100 g, 1.6 mmol), EtOH (5.0 mL) and H_2O (1.0 mL) was heated at 150 °C for 20 min. The colorless crystals of **2** were filtered off, washed with EtOH, dried at room temperature, and collected with the yield of 0.0720 g (41.21%, based on the H_2SBA reagent). Anal. found/calcd.: C, 41.77/41.00; H, 3.99/4.24% for **2**. IR (KBr, cm^{-1}): 3531(w), 3268(w), 2978(w), 1620(s), 1564(m), 1413(s), 1291(m), 1165(m), 1102(m), 789(w), 746(s), 698(w), 621(w), 491(w), 442(w).

Microwave synthesis of $[Ni_3(OH)_2(SBA)_2(EtOH)(H_2O)_3]\cdot 3.5H_2O$ (3). The compound **3** was obtained from a reaction mixture of H_2SBA (0.0612 g, 0.2 mmol), $NiCl_2\cdot 6H_2O$ (0.0475 g, 0.2 mmol), DMF (3.0 mL), (EtOH, 7.0 mL), and H_2O (1.0 mL). The mixture was heated at 180 °C for 20 min. The green crystals of **3** were filtered off, washed with EtOH, dried at room temperature, and collected with the yield of 0.0425 g (43.41%, based on the H_2SBA reagent). Anal. found/calcd.: C, 36.92/36.84; H, 3.48/3.53% for **3**. IR (KBr, cm^{-1}): 3525(m), 3226(b), 1680(s), 1608(s), 1569(s), 1482(s), 1285(s), 1156(s), 1104(s), 1011(s), 743(s), 684(s), 628(s), 490(s), 422(s).

Microwave synthesis of $[Co_3(OH)_2(SBA)_2(EtOH)(H_2O)_3]\cdot 3.5H_2O$ (4). The compound **4** was obtained from a reaction mixture of H_2SBA (0.0612 g, 0.2 mmol), $CoCl_2\cdot 6H_2O$ (0.0475 g, 0.2 mmol), DMF (3.0 mL), EtOH (7.0 mL), and H_2O (1.0 mL). The mixture was heated at 150 °C for 20 min. The pink crystals of **4** were filtered off, washed with EtOH, dried at room temperature, and collected with the yield of 0.0503 g (51.23%, based on the H_2SBA reagent). Anal. found/calcd.: C, 36.79/36.67; H, 3.82/3.80% for **4**. IR (KBr, cm^{-1}): 3529(m), 3224(b), 1682(s), 1601(s), 1572(s), 1480(s), 1159(s), 1101(s), 741(s), 624(s), 493(s), 425(s).

Microwave synthesis of [Mn(SBA)(EtOH)] (5). The compound **5** was obtained from a reaction mixture of H_2SBA (0.1224 g, 0.4 mmol), $Mn(NO_3)_2\cdot 4H_2O$ (0.2000 g, 0.8 mmol), EtOH (5.0 mL) and H_2O (1.0 mL). The mixture was heated at 180 °C for 20 min. Only very few light-pink crystals of **5** were collected.

Microwave synthesis of [Mn(SBA)(H_2O)] (6). The compound **6** was obtained from a reaction mixture of H_2SBA (0.2448 g, 0.8 mmol), $Mn(NO_3)_2\cdot 4H_2O$ (0.2000 g, 0.8 mmol), EtOH (7.0 mL), and H_2O (3.0 mL). The mixture was heated at 180 °C for 20 min. Only very few colorless crystals of **6** were collected.

Preparation of desolvated phases, $[M_3(OH)_2(SBA)_2]$ (CYCU-5 and 2a–4a). The heating of as-synthesized compounds **1–4** at 200 °C for 10 h resulted in the desolvated phases (**CYCU-5** and **2a–4a**).

Single-crystal structure analysis

The diffraction measurements were performed on a Bruker AXS SMART APEX II diffractometer (Mo-Kα radiation, graphite monochromator, λ = 0.71073 Å). All data were corrected for Lorentz and polarization effects, and the program *SADABS* in *APEX2* (ref. 15) was used for the absorption correction. On the basis of systematic absences and statistics of intensity distribution, all the single crystal structures were solved with metal atoms being located first, followed by the atoms O, N, and C located on successive difference Fourier maps. The H atoms were added in idealized positions and constrained to ride on their parent atoms. All calculations were performed by using *SHELXTL* programs in *APEX2*.[16] While the framework structure of **1** was refined easily, the solvent molecules in **1** could not be refined because of their highly disordered structure. Therefore, the SQUEEZE function of the PLATON program was used to eliminate the contribution of the electron density in the solvent region from the intensity data. Crystallographic data are given in Table 1. Selected bond lengths are listed in Table S1 (ESI†). Crystallographic data (CIF) for the single crystal structures reported in this paper have been deposited with the Cambridge Crystallographic Data Centre (CCDC) as supplementary publication numbers CCDC 943771, 943772, 805748, 998723, and 998724 for the compounds, **1**, **CYCU-5**, **2**, **5**, and **6**, respectively.

Structural matching and Powder X-Ray Diffraction (PXRD) analysis

The powder X-ray diffraction (PXRD) patterns were also recorded at the BL01C2 beamline of the National Synchrotron Radiation Research Center (NSRRC) in Taiwan. The ring energy of NSRRC was operated at 12 keV with a typical current of 300 mA. The wavelength of the incident X-rays was 1.0332 Å, delivered from the superconducting wavelength-shifting magnet, and a Si(111) double-crystal monochromator. The diffraction patterns were recorded with a Mar345 imaging plate detector approximately 280 mm from sample positions and typical exposure duration of 5 min. The pixel size of Mar345 was 100 μm. The one-dimensional powder diffraction profile was converted with the program FIT2D and cake-type integration. The diffraction angles were calibrated according to Bragg positions of Ag-benhenate and Si powder (NBS640b) standards. The powder sample was sealed in a capillary (0.7 mm diameter) and heated in a stream of hot air. The Rietveld refinements of all powder samples were carried out with the GSAS program.[17] Crystallographic details of the compounds determined from synchrotron PXRD data are given in Tables 2 & 3 and S4 (ESI†). Selected bond lengths are listed in Tables S5 and S6 (ESI†). The Rietveld plot corresponds to the crystal structure model and profile factors are displayed in Fig. S7 and S8 (ESI†). Crystallographic data (CIF) for the powder samples structural refinements are published as ESI.†

Results and discussion

Structural description of $[Zn_3(OH)_2(SBA)_2]\cdot EtOH$ (1 or CYCU-5·EtOH)

Single crystal X-ray diffraction structure analysis shows that the structure of the compound **1** possesses an extended 2D framework. The asymmetric unit consists of two crystallographically independent Zn centers and two SBA ligand units (Fig. 1a). The Zn(1) center is six-coordinated and bonded to four oxygen atoms of the carboxylate groups belonging to

Table 1 Single crystal crystallographic data

	1	CYCU-5	2	5	6
Formula	$C_{15}H_{12}Zn_{1.5}O_{7.5}S$	$C_{14}H_9Zn_{1.5}O_7S$	$C_{30}H_{37}Mg_3O_{21.5}S_2$	$C_{16}H_{13}MnO_7S$	$C_{14}H_{10}MnO_7S$
Fw	442.36	419.33	878.65	404.26	377.22
Space group	$P2_1/n$	$P2_1/n$	$P2/c$	$P2_1/n$	$P\bar{1}$
a (Å)	14.0847(4)	14.1168(2)	28.1637(9)	10.1610(5)	5.998(2)
b (Å)	5.9953(2)	6.0531(10)	6.441(2)	7.3197(3)	11.8959(4)
c (Å)	19.3347(6)	19.3678(3)	24.8679(8)	22.3295(10)	13.0287(7)
α (°)	90	90	90	90	112.118(3)
β (°)	93.729(2)	93.627(10)	115.445(2)	93.6990(10)	102.502(3)
γ (°)	90	90	90	90	99.816(2)
V (Å^3)	1629.20(9)	1651.67(4)	4073.6(2)	1657.31(13)	807.49(6)
Z	4	4	4	4	2
D_{calc} (g cm^{-3})	1.803	1.686	1.433	1.620	1.551
μ (mm^{-1})	2.393	2.353	0.28	0.959	0.978
Reflections collected	26 234	15 157	45 162	14 612	13 815
Independent reflections	4029	4098	10 210	4090	3960
R(int)	0.0337	0.0300	0.0806	0.0381	0.0344
Goodness-of-fit on F^2	1.147	0.979	1.037	1.165	1.082
R_1 [$I > 2\sigma(I)$]	0.0459	0.0301	0.0541	0.0572	0.0492
wR_2 [$I > 2\sigma(I)$]	0.1146	0.0709	0.1468	0.1548	0.1241
R_1 [all data]	0.0508	0.0470	0.1118	0.0630	0.0601
wR_2 (all data)	0.1167	0.0785	0.1672	0.1573	0.1282
CCDC no.	943771	943772	805748	998723	998724

Table 2 Crystallographic details of **3** and **4** at 303 K, as determined from synchrotron PXRD data

	3 (83%)	**3a** (17%)	**4**
Chemical formula	$C_{30}H_{29}Ni_3O_{18}S_2$	$C_{28}H_{18}Ni_3O_{14}S_2$	$C_{30}H_{29}Co_3O_{18}S_2$
Formula weight	914.89	815.8	917.88
Crystal system	Monoclinic	Monoclinic	Monoclinic
Temperature (K)	303	303	303
Space group	*P*2/*c*	*P*2$_1$/*n*	*P*2/*c*
a (Å)	27.051(7)	12.738(6)	28.1888(19)
b (Å)	6.2522(14)	6.240(6)	6.3545(3)
c (Å)	24.945(8)	21.545(8)	24.9584(15)
β (°)	115.191(12)	89.61(5)	115.737(4)
V (Å^3)	3817.66(183)	1712.47(219)	4027.2(4)
Z	4	2	4
Radiation (Å)	1.0332	1.0332	1.0332
χ^2	6.332	6.332	2.346
R_p (%)	5.31	5.31	4.64
R_{wp} (%)	7.53	7.53	7.08

four SBA units, and the remaining two octahedral coordination sites, which are '*trans*' to each other, have been occupied by two oxygen atoms (O3) of the two hydroxide ions. On the other hand, the tetrahedrally four-coordinated Zn(2) atom is coordinated with two oxygen atoms of the carboxylate groups belonging to two SBA ligand units, and two oxygen atoms (O3) of the two hydroxide ions. The hydroxide ions act as a bridge to connect the Zn(1) and Zn(2) centers. The SBA ligand is tetradentate, bridging to four Zn centers through each of its four carboxylate oxygen atoms (Fig. 1b). All of the Zn–O bond distances range from 1.909(3) to 2.170(3) Å (Table S1, ESI†). As shown in Fig. 1c, the inorganic motif displays 1D chains formed by the edge-sharing Zn_2O_{10} and corner-sharing ZnO_6. The one-dimensional inorganic building unit in compound **1** has been reported previously for a zinc terephthalate open framework.[18] These chains are linked together by the μ_4-links of SBA ligands in two directions to generate the 2D metal–organic framework of **1** (Fig. 1d). The layers interact further by hydrogen bonds (Table S2, ESI†). The framework contains rhomboidal channels with a free diameter of 5.1 × 4.7 Å^2 (considering the van der Waals radii of atoms) without including the water and EtOH molecules. The solvent accessible volume (SAV) calculated without including ethanol and water molecules by PLATON[19] analysis is 301.7 Å^3 which is 18.5% of the unit cell volume.

Structural description of $[M_3(OH)_2(SBA)_2(EtOH)(H_2O)_3]\cdot 3.5H_2O$ (2–4, M = Mg, Ni, Co)

Single crystal X-ray structure analysis of compound **2** and PXRD fitting of compounds **3** and **4** displayed that compounds **2** to **4** have similar conformations to $[Co_3(OH)_2(SBA)_2(EtOH)(H_2O)_3]\cdot 3.5H_2O$,[13] which was synthesized by conventional heating. For **2**, all of the Mg–O bond distances range from 2.049(2) to 2.124(2) Å (Fig. 2a, Table S1, ESI†). The layer structure of **2** (Fig. 2b) consists of $[Mg_3(\mu_3\text{-}OH)_2]_n$ chains linked by SBA ligands. In the chain, the Mg atoms, Mg(1), Mg(2) and Mg(3) are first linked by one μ_3-OH. Along the chain direction (*b*-axis) these three magnesium centers are further connected by another μ_3-OH. Within the 1D chains, the $Mg(2)O_6$ and $Mg(3)O_6$ octahedra are edge-sharing, and they are apex-shared with the $Mg(1)O_6$ octahedra (Fig. 2c). The layers are further connected by hydrogen bonds between the coordinated water molecules and oxygen atoms on the sulfone group (Table S2, ESI†). Each layer contains rhomboidal channels with a free diameter of 5.2 × 4.7 Å^2 (considering the van der Waals radii of atoms) without including the water and EtOH molecules. The SAV calculated without including ethanol and water molecules by PLATON[19] analysis is 1319.4 Å^3, which is 32.4% of the unit cell volume. The comparison of this hypothetical calculation with the results of **CYCU-5** clearly indicates that if the solvent molecules of **2** are removed without structural transformation or distortion, this leads to a larger free pore volume.

Structural description of [Mn(SBA)(EtOH)] (5)

Single crystal structure analysis shows that the structure of the compound **5** also possesses an extended 2D framework. The asymmetric unit consists of one crystallographically independent Mn center, one SBA ligand, and one EtOH

Table 3 Crystallographic details of **CYCU-5** and **2a**–**4a** at 473 K, as determined from synchrotron PXRD data

	CYCU-5	**2a**	**3a**	**4a**
Chemical formula	$C_{28}H_{18}Zn_3O_{14}S_2$	$C_{28}H_{18}Mg_3O_{14}S_2$	$C_{28}H_{18}Ni_3O_{14}S_2$	$C_{28}H_{18}Co_3O_{14}S_2$
Formula weight	833.8	714.0	815.8	818.8
Crystal system	Monoclinic	Monoclinic	Monoclinic	Monoclinic
Temperature (K)	473	473	473	473
Space group	*P*2$_1$/*n*	*P*2$_1$/*n*	*P*2$_1$/*n*	*P*2$_1$/*n*
a (Å)	13.9323(6)	14.307(21)	13.9069(32)	13.881(14)
b (Å)	6.0385(2)	6.082(5)	6.1607(10)	6.1930(26)
c (Å)	19.3839(8)	18.816(17)	19.288(7)	20.006(13)
β (°)	93.2021(22)	89.325(11)	90.30(4)	90.0(1)
V (Å^3)	1628.3(2)	1637.16(313)	1652.5(8)	1719.82(219)
Z	2	2	2	2
Radiation (Å)	1.0332	1.0332	1.0332	1.0332
χ^2	2.653	3.425	6.479	4.447
R_p (%)	2.49	6.74	5.55	6.818
R_{wp} (%)	4.54	9.90	9.03	9.90

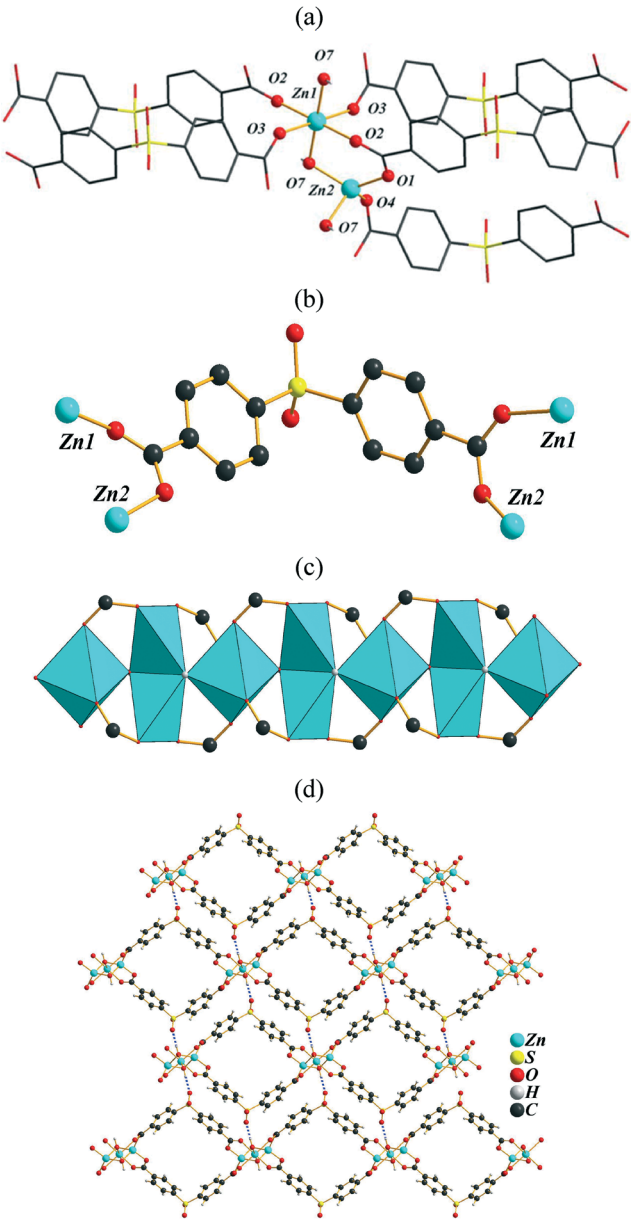

Fig. 1 (a) The coordination spheres of zinc atoms in **1**. (b) The coordination environment of the SBA ligand. (c) The edge-sharing and corner-sharing 1D inorganic chain in **1**. (d) The 2D structure view of **1** with the channels along the *b*-axis.

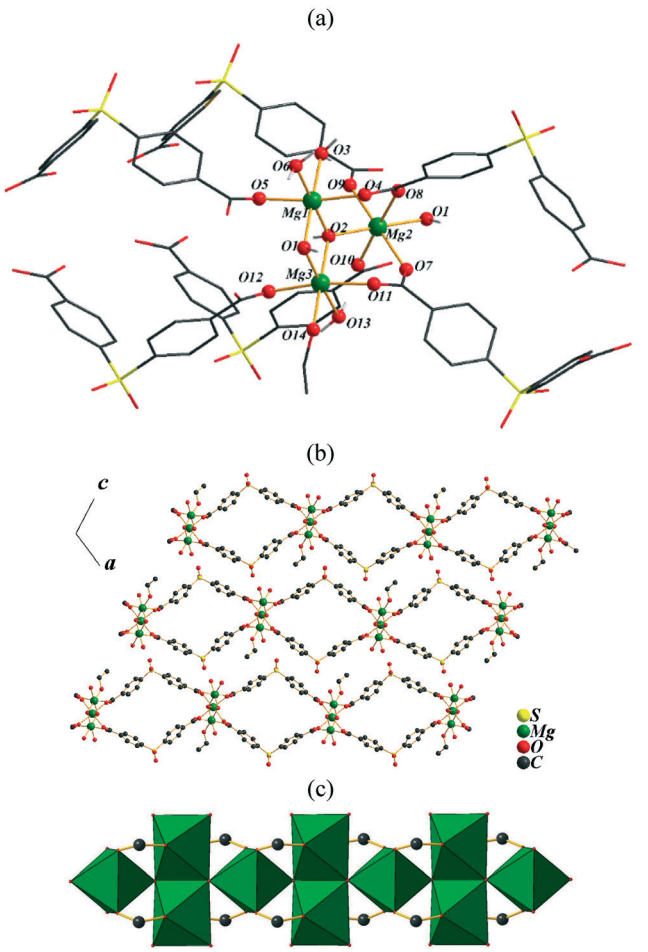

Fig. 2 (a) The coordination spheres of magnesium atoms in **2**. (b) The 2D structure view of **2** with the channels along the *b*-axis. (c) The edge-sharing and corner-sharing 1-D inorganic chain in **2**.

(Fig. 3a). The Mn(II) ion is six-coordinated and bonded with five oxygen atoms from the carboxylate groups belonging to four SBA ligands, and one oxygen atom from the coordinated EtOH molecule. The SBA ligand has acts as pentadentate and is coordinated with four Mn centers (Fig. 3b) through its carboxylate oxygen atoms. The Mn–O bond distances range from 2.085(3) to 2.369(3) Å (Table S1, ESI†). As shown in Fig. 3c, the inorganic motif displays 1D chains, formed by the corner-sharing MnO_6 polyhedra. These chains are linked together by the SBA ligands in two directions to generate the 2D metal–organic framework of **5** (Fig. 3d). The framework of **5** contains rhomboidal channels with a free diameter of 5.9 × 5.3 $Å^2$ (considering the van der Waals radii of atoms) without including the water and EtOH molecules. The SAV calculated without including ethanol molecules by PLATON[19] analysis is 374.2 $Å^3$, which is 22.6% of the unit cell volume. This value is comparable to that of **CYCU-5**.

Structural description of [Mn(SBA)(H_2O)] (6)

Single crystal X-ray diffraction shows that the structure of the compound **6** also possesses an extended 2D framework. The asymmetric unit consists of one independent Mn center, one SBA ligand, and one coordinated water molecule (Fig. 4a). The Mn(II) ion is six-coordinated and binds with six oxygen atoms from the carboxylate groups belonging to five H_2SBA ligands, and one oxygen atom from the coordinated water molecule. The H_2SBA ligand overall is pentadentate, bridging with five Mn(II) ions through each of its five carboxylate oxygen atoms (Fig. 4b). The Mn–O bond distances range from 2.126(2) to 2.284(2) Å (Table S1, ESI†). As shown in Fig. 4c, the inorganic motif displays 1D chains, which are formed by the edge-sharing Mn_2O_{10} that are connected by SBA ligand units. These chains are further linked together by the μ_5-links

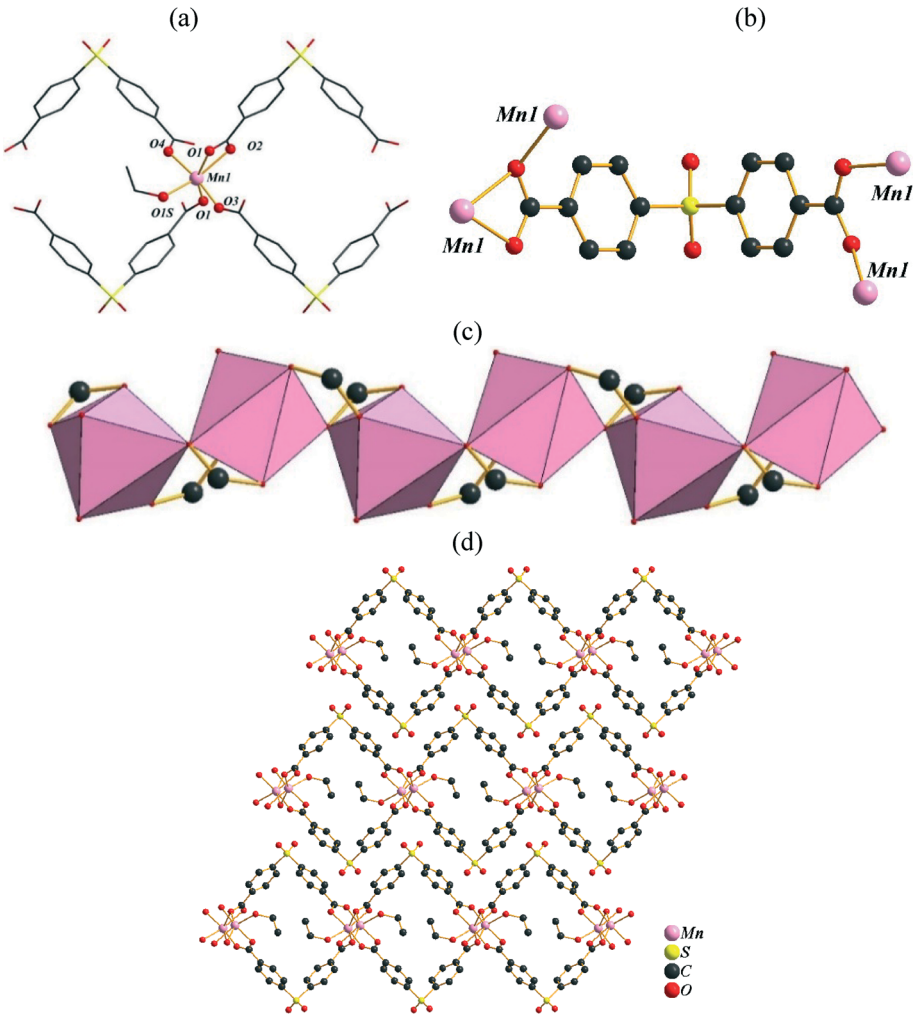

Fig. 3 (a) The coordination sphere of Mn in **5**. (b) The coordination environment of the SBA ligand in **5**. (c) The corner-sharing 1D inorganic chain in **5**. (d) The 2D structure view of **5** with the channels along the *b*-axis.

of SBA ligands in two directions to generate the 2D metal–organic framework of **6** (Fig. 4d). The framework contains rhomboidal channels with a free diameter of 5.6 × 5.0 $Å^2$ (considering the van der Waals radii of atoms) without including the water molecules. The SAV calculated without including water molecules by PLATON[19] analysis is 129.6 $Å^3$, which is 16.1% of the unit cell volume. The lower number of coordinated solvent molecules in the structure reduces the possible free volume in compound **6**.

Evaluation of structural transformation

It is interesting to note that the various temperature PXRD patterns of **1** displayed similar patterns up to 673 K (Fig. S2, ESI†), which indicates the SBUs of inorganic chains remain stable with ZnO_4 tetrahedra and ZnO_6 octahedra under high temperature (673 K). All these PXRD patterns were evaluated in detail by carrying out Rietveld profile fitting (Fig. 5 and S7, ESI†), which displayed that the lattice parameters change upon activation (Fig. 6). The results showed a trend for increasing lattice parameter values along the *a*- and *b*-axes as temperature increased, while the *c*-axis showed decreasing values after 423 K. The unit cell volume generally expanded when the temperature was increased. As shown in Table S6 (ESI†), two bond lengths (Zn2–O2 and S1–O4) and one distance (O1···O4) are consistent with the variation of the *c*-axis. Both tetrahedral distortion and hydrogen bonding could explain the structural transformation well.

All desolvated samples of **2a–4a** are isostructural and have the same structure as in activated **1**, with a monoclinic crystal system and $P2_1/n$ space group (Fig. 7). In **2–4**, the first two peaks in the PXRD pattern transfer to **2a–4a** with one main peak at 473 K, which may be corresponding to the solvent removal and the structural transformation to CYCU-5-like frameworks (Fig. S3–S5, ESI†). However, a few extra phases (intermediate phases) have been observed in the varied temperature PXRD patterns of **3** at 303–473 K and **4** at 373 K (Fig. S4 and S5, ESI†), which were structurally identified as as-synthesized and desolvated phases. The Rietveld profile fits to synchrotron PXRD data for **3** and **4** showed that the percentage ratio of as-synthesized and desolvated phases are 83 : 17 and 67 : 33 respectively. For **2a–4a**, as shown in Table S7 (ESI†), the bond length (M2–O2) relative to tetrahedral

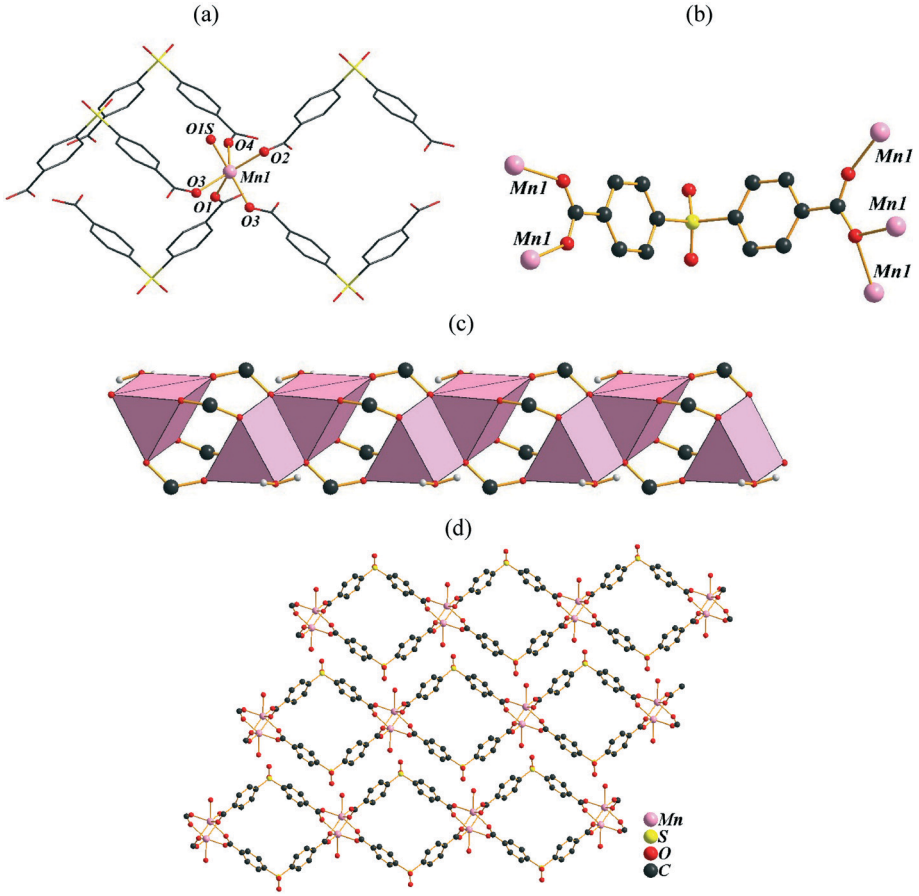

Fig. 4 (a) The coordination sphere of the Mn atom in **6**. (b) The coordination environment of the SBA ligand in **6**. (c) The edge-sharing and corner-sharing 1D inorganic chain in **6**. (d) The 2D structure view of **6** with the channels along the *b*-axis.

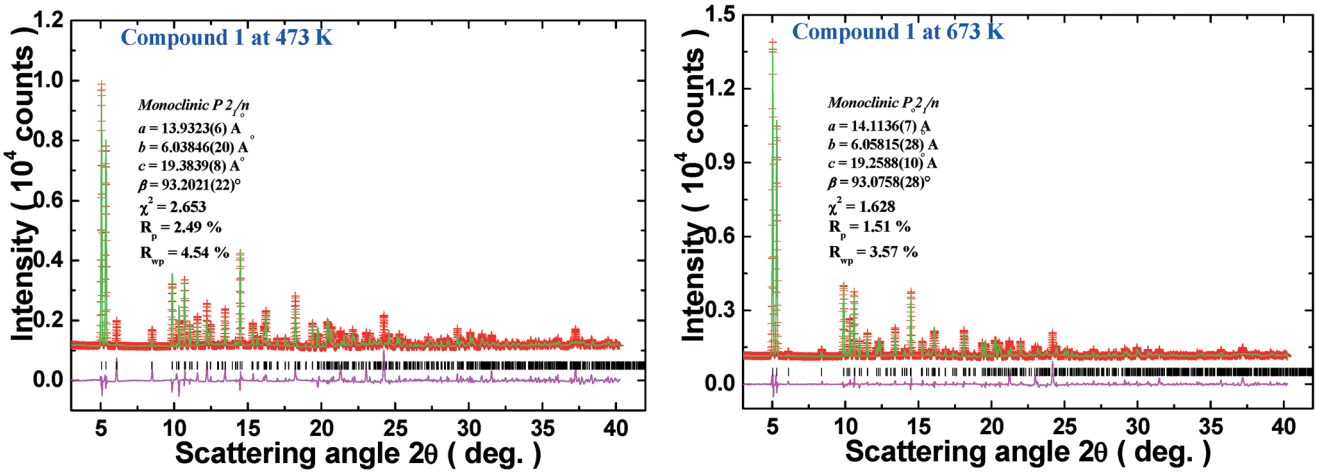

Fig. 5 Rietveld profile fits to synchrotron PXRD data for **CYCU-5** at 473 K and 673 K. The measured values are in red, the calculated intensity is in green and the difference plot is in pink.

distortion and both the bond length (S1–O4) and distance (O1···O4) relative to hydrogen bonding are the main considerations during the structural transformation. Finally, the PXRD patterns of **CYCU-5** and **2a–4a** at 473 K were well fitted and reveal that the activated frameworks should have similar conformations.

Thermogravimetric analysis

Thermogravimetric analyses (TGA) were performed to determine the thermal stabilities of the studied compounds **1–4** (Fig. S1, ESI†), and their corresponding weight losses of solvent molecules at the different temperatures with their

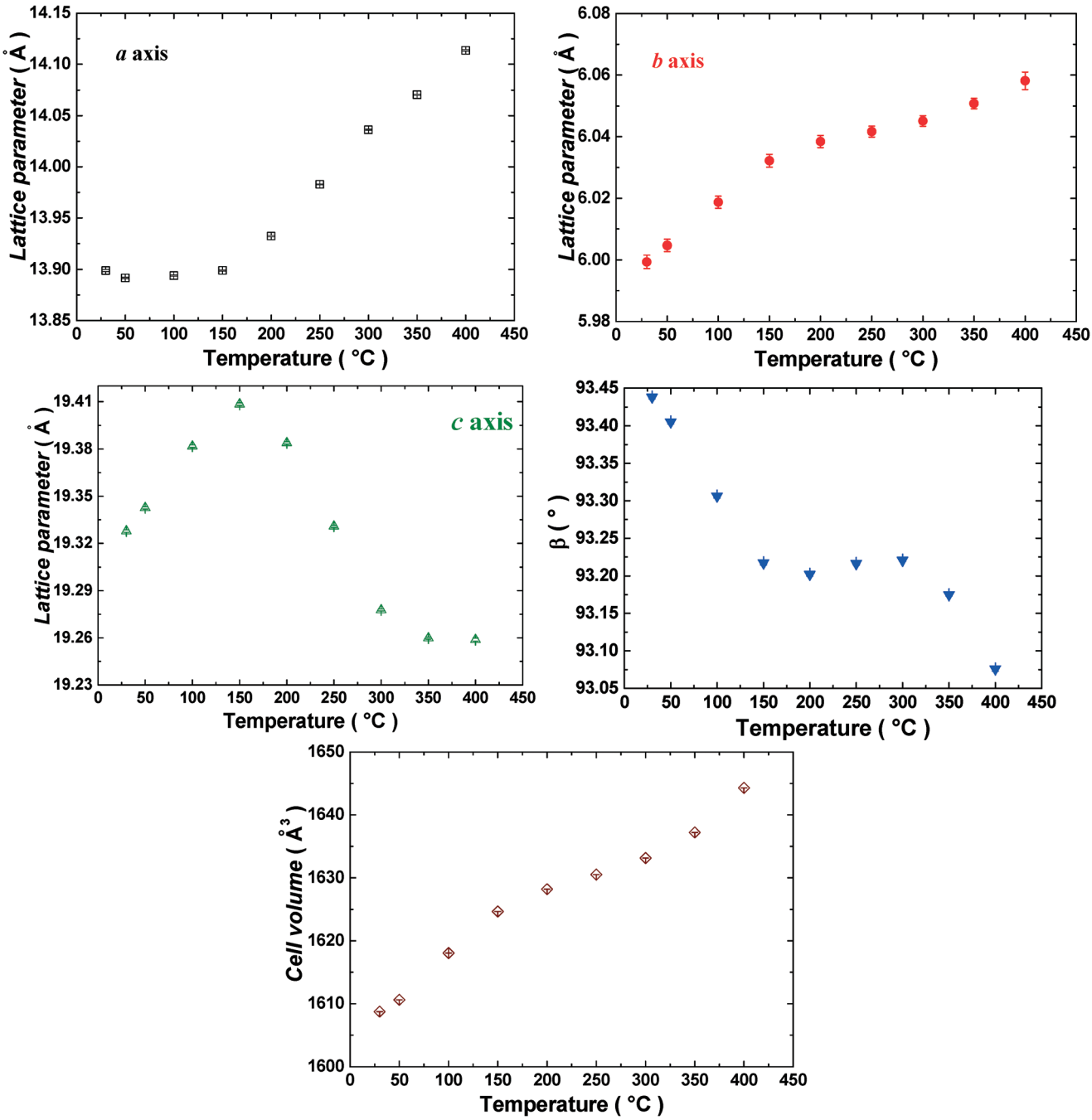

Fig. 6 Final Rietveld refinement lattice parameters for **1** at various temperatures.

calculated weight losses are tabulated (Table S3, ESI†). The TGA curve of **1** showed the first gradual weight loss of about 6% up to 300 °C, corresponding to the release of the crystallized ethanol molecule (*ca.* 5.2%). So, the CYCU-5 was thermally stable up to about 400 °C. The further weight loss up to 800 °C might correspond to the decomposition of organic ligands, which form zinc oxide (Fig. S7, ESI†). The TGA curve of **2** revealed that all the water and ethanol molecules are easily removed in two steps slightly above 150 °C, and the mass loss of 18.1% agrees well with the calculated 16.8%; it might lose its lattice water molecules in the first step, followed by the loss of coordinated water and ethanol molecules in the second step. Further, the desolvated phase, $[Mg_3(OH)_2(SBA)_2]$ was fairly stable up to 400 °C, then the framework of **2** started to decompose. The TGA curves of compounds **3** and **4** have shown similar thermal stability behaviors to those seen in **2**. That is, the water and ethanol molecules removal occurred in two steps at around 200 °C and 120 °C for the compounds **3** and **4**, respectively. It is noteworthy to mention that the desolvated phases of **3** and **4** are thermally stable up to 350 °C. Further heating of the compounds up to 800 °C results in decomposition of framework structures. As

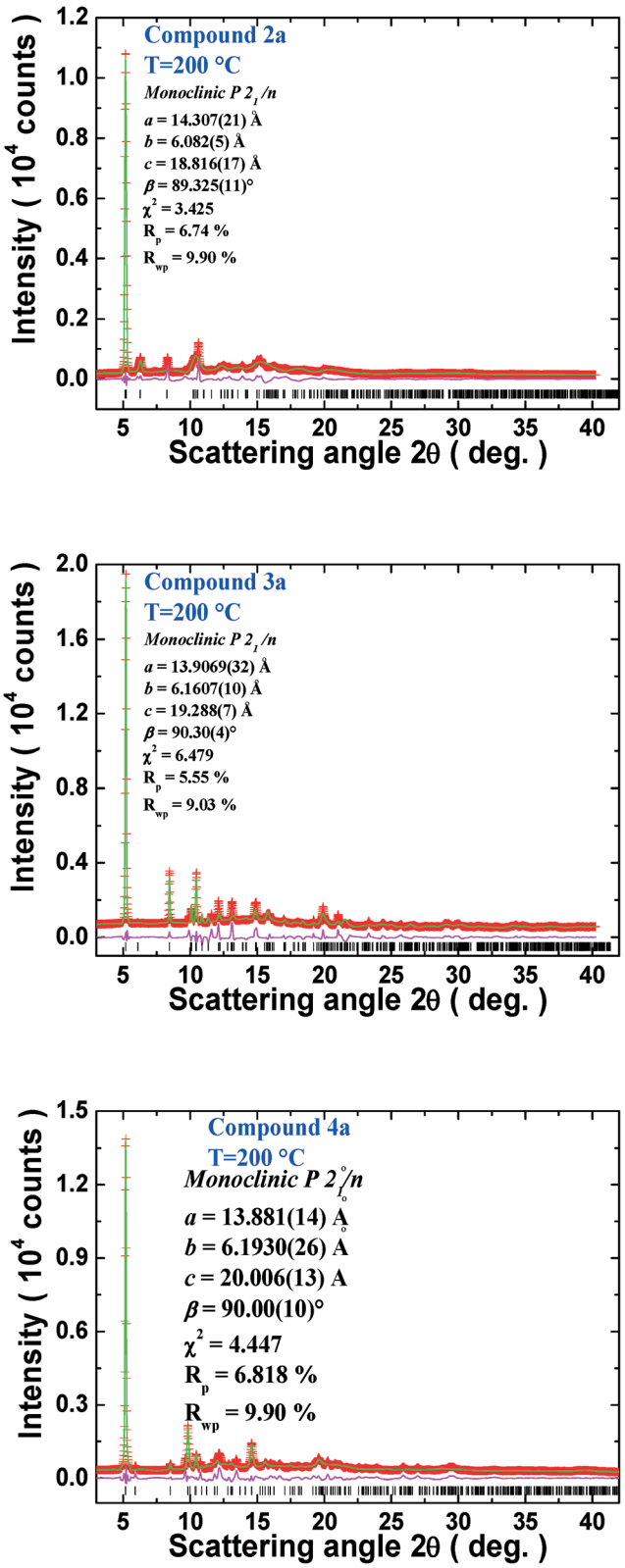

Fig. 7 Final Rietveld-plot for **2a–4a** at 473 K. The measured values are in red, the calculated intensity is in green and the difference plot is in pink.

displayed in Fig. S8 (ESI†), the Rietveld profile fits of synchrotron PXRD data for **4** at 673 K show the existence of three types of cobalt oxides.

Gas sorption properties

To verify the porosity of the guest-free phase of compounds **1–4** (**CYCU-5**, **2a–4a**), gas sorption isotherms have been measured with N_2, CO_2 and H_2. The N_2 gas adsorption isotherm at 77 K for the compounds shows type-I behavior with a steep rise in the very low pressure region, suggesting a microporous nature. The N_2 gas sorption results of compounds **CYCU-5**, **2a–4a** are tabulated in Table 4. From the results obtained from the N_2 gas sorption experiments (Fig. 8), it has been found that compound **4a** has better N_2 gas sorption capacity than that of the other three (**CYCU-5**, **2a** and **3a**).

In the case of the CO_2 adsorption isotherms for the compounds at 273 and 298 K (Fig. 9), the compounds showed moderate CO_2 adsorption behavior and their corresponding values are depicted in Table 5. All the compounds showed better CO_2 uptake at low temperature (273 K) than at room temperature (298 K). Compound **4a** showed the highest CO_2 uptake among the four as we have seen in the N_2 case also. The results of the CO_2 uptake for the compounds are comparable with some of the reported compounds, Zn_2(tetrakis[4-(carboxyphenyl)oxamethyl]methane)(4,4′-bipyridine)[20] and MOF-5/IRMOF-1 (ref. 21), under similar conditions.

On the other hand, the H_2 gas sorption properties of the compounds have been studied at 77 K (Fig. 10). All four compounds showed some amount of H_2 uptake at 1 atm, given in Table 5. Like in the previous two cases, compound **4a** exhibited better H_2 storage capacity among the four compounds studied. Surprisingly, **CYCU-5** displayed almost no

Table 4 The N_2 gas sorption data of **CYCU-5**, **2a–4a**

Compound	BET surface area ($m^2\ g^{-1}$)	Langmuir surface area ($m^2\ g^{-1}$)
CYCU-5	19.6	24.1
2a	44.5	59.9
3a	9.7	11.7
4a	71.5	92.6

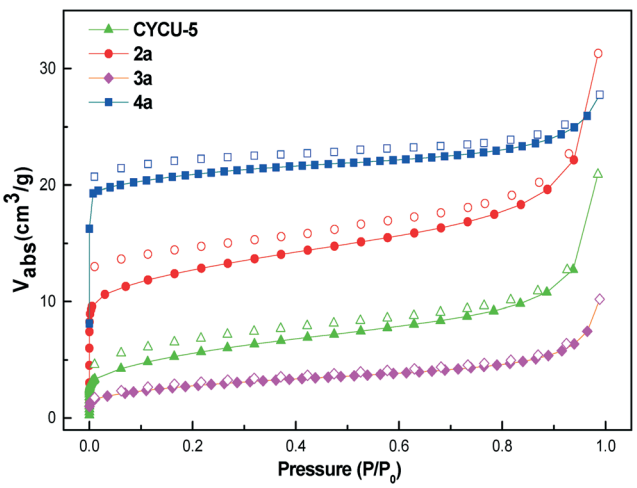

Fig. 8 Nitrogen adsorption isotherms for the compounds, **CYCU-5**, **2a–4a**.

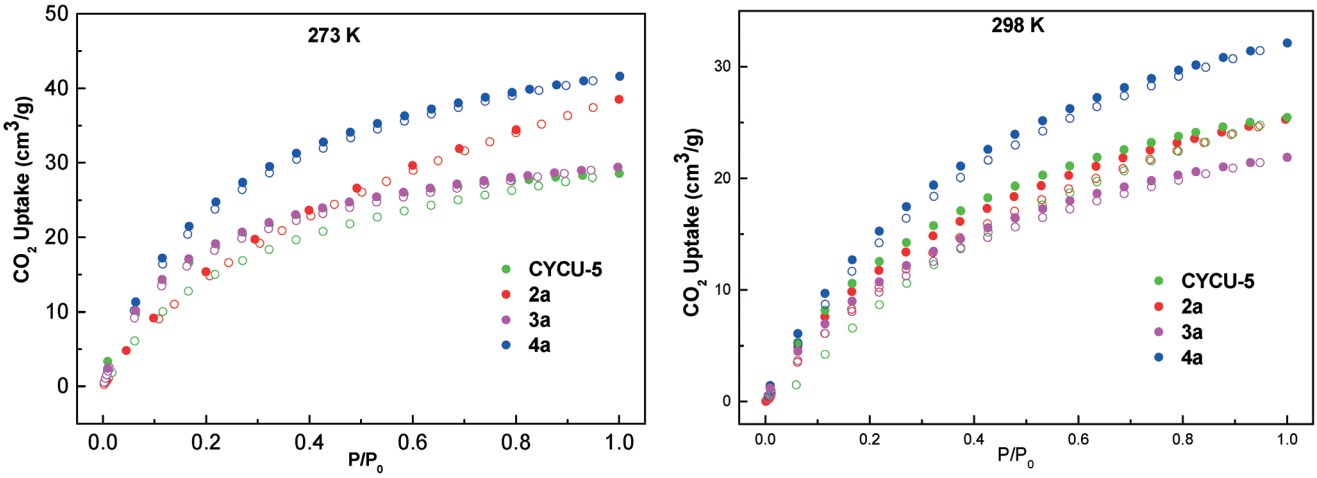

Fig. 9 The CO_2 adsorption isotherms for the compounds **CYCU-5** and **2a–4a**, measured at 273 K and 298 K.

Table 5 The CO_2 and H_2 uptake data of **CYCU-5**, **2a–4a**

Compounds	CO_2 uptake in $cm^3\ g^{-1}$ ($mmol\ g^{-1}$) at 1 atm		H_2 uptake at 77 K, 1 atm in $mmol\ g^{-1}$ (wt.%)
	273 K	298 K	
CYCU-5	29.39 (1.31)	21.87 (0.98)	0.44 (0.09)
2a	38.52 (1.72)	25.28 (1.13)	1.63 (0.32)
3a	28.54 (1.27)	25.46 (1.14)	1.49 (0.30)
4a	41.62 (1.86)	32.11 (1.43)	1.96 (0.39)

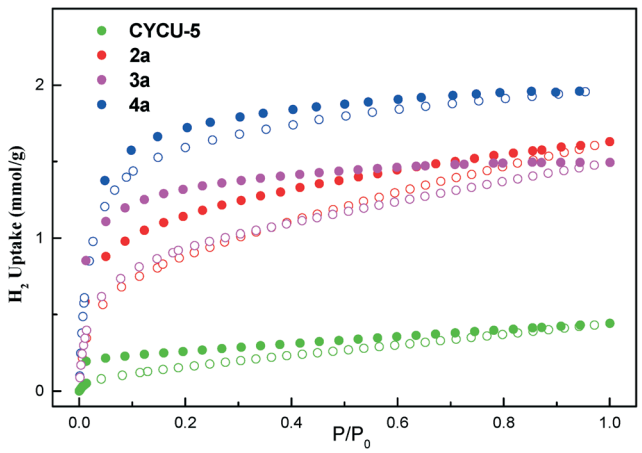

Fig. 10 The H_2 adsorption–desorption isotherms of **CYCU-5**, **2a–4a**, at 77 K.

H_2 gas sorption capacity. The H_2 gas sorption capacity of **4a**, **3a** and **2a** are comparable with the reported compounds [Cu(hfipbb)($h_2$hfipbb)$_{0.5}$],[22] PCN-13,[23] [Mn(NDC)],[24] and $[Cd_2(Tzc)_2]$[25] under similar conditions.

In order to explore the potential gas separation properties of **CYCU-5** under ambient conditions, the adsorption isotherms of CO_2, N_2, and CH_4 for **CYCU-5** at 273 K were measured (Fig. 11). The CO_2 uptake value at 1 atm is 5.00 wt.% at

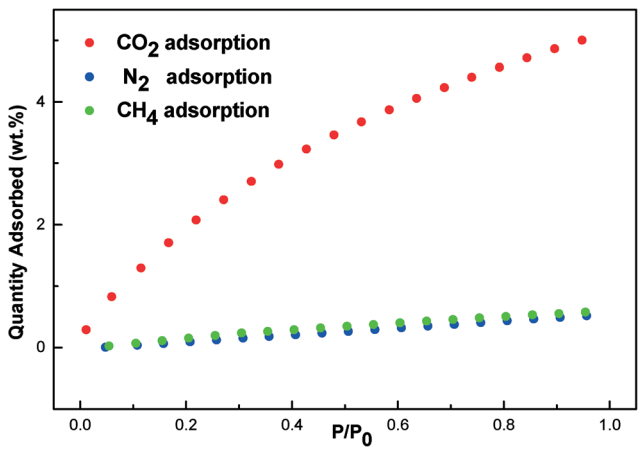

Fig. 11 CO_2, N_2, and CH_4 gas uptake of **CYCU-5** at 273 K.

273 K, which is much higher than those of N_2 (0.51 wt.%), and CH_4 (0.58 wt.%). Hence, the above values clearly suggest that **CYCU-5** has selective CO_2 gas adsorption over N_2 and CH_4 gases at similar conditions. The selective CO_2 adsorption over the other gases for **CYCU-5** can be ascribed to the quadrupole moment of CO_2 (-1.4×10^{-39} C m^2),[26] which induces an interaction with the framework.[27] By fitting the CO_2 adsorption data of **CYCU-5** to the Dubinin–Radushkevich (DR) equation, the surface area was determined to be 36.4 $m^2\ g^{-1}$.

Further, the high pressure CO_2 and CH_4 adsorption isotherms of **CYCU-5** at 273 and 298 K have been measured (Fig. S10, ESI†). The results indicate that **CYCU-5** has a maximum CO_2 adsorption of 94.8 $cm^3\ g^{-1}$ (at 33.5 bar, and 273 K) and 58.5 $cm^3\ g^{-1}$ (at 39.4 bar, and 298 K). However, the maximum CH_4 uptake of **CYCU-5** at 89 bar pressure, is 110 $cm^3\ g^{-1}$ (at 273 K) and 49.9 $cm^3\ g^{-1}$ (at 298 K). In order to see the stability of the compounds after gas sorption experiments, PXRD was carried out for the compounds before and after gas sorption studies. The PXRD patterns of the compounds after gas

Table 6 Results of the ROP of L-LA using compound **CYCU-5** as a catalyst

Entry	$[L\text{-}LA]_0/[Cat.]_0$	Toluene (mL)	Conv.[b] (%)	M_n[c] (calcd.)	M_n[d] (obsd.)	PDI[e]
1[a]	100/1	0	78	11 278	40 100 (23 300)	1.70
2[a]	100/1	5	34	4942	3900 (2262)	1.06
3[a]	100/1	1	47	6814	15 600 (9048)	1.15

[a] $[Cat.]_0$ = 88 mg (0.1 mmol), 140 °C, 72 h. [b] Obtained from ^1H NMR determination. [c] Calculated from the molecular weight of lactic acid × $[L\text{-}LA]_0/[Cat.]_0$ × conversion yield. [d] Obtained from GPC analysis and calibrated by polystyrene standard. Values in parentheses are the values obtained from GPC × 0.56. [e] Obtained from GPC analysis.

sorption studies (Fig. S6, ESI†) indicated that the frameworks of all the compounds were stable after the gas sorption experiments.

Catalytic properties

Though MOFs are well-known for their catalytic activities for various reactions, it is much less common to explore the catalytic activity of a MOF in ring-opening polymerization (ROP) of L-lactide (L-LA).[28] Hence, the catalytic activity of **CYCU-5** as an initiator in the ROP of L-LA has been evaluated and the representative results are outlined in Table 6. It has been noted that 78% of conversion has been observed without using toluene solvent (entry 1, Table 6). The results indicated that **CYCU-5** has moderate catalytic activity for the ROP of L-LA at some particular reaction conditions. Even though the catalytic activity results of **CYCU-5** are not very promising, it is one of the few porous MOFs having a catalytic performance for the ROP of L-LA.

Conclusions

In summary, we have successfully synthesized six 2D metal–organic frameworks under microwave-assisted solvothermal reaction conditions, based on a rigid V-shaped 4,4′-sulfonyldibenzoic acid (H_2SBA) ligand. The compounds contain 1D open channels inside the 2D frameworks, which are constructed from 1D inorganic chain SBUs. The various temperature PXRD patterns of **1–4** suggested that the desolvated frameworks of **1–4** above 473 K have similar **CYCU-5**-like conformations with high thermal stabilities. Compounds **1–4** demonstrated impressive gas adsorption capacities for CO_2 and H_2. The gas adsorption behavior of **CYCU-5** displayed selective CO_2 gas adsorption over N_2 and CH_4 gases at 273 K. Further, **CYCU-5** demonstrated preliminary catalytic activity for the ring-opening polymerization reaction of L-lactide.

Acknowledgements

Financial assistance received from the Ministry of Science and Technology, Taiwan (NSC 101-2113-M-033-007-MY3 and MOST 103-2632-M-033-001-MY3) is gratefully acknowledged. Acknowledgment is also made to Mrs. C.-W. Lu, Instrumentation Center, National Taiwan University, Taiwan for her help in elemental analyses.

References

1 (*a*) M. Eddaoudi, D. B. Moler, H. Li, B. Chen, T. M. Reineke, M. O'Keeffe and O. M. Yaghi, *Acc. Chem. Res.*, 2001, **34**, 319; (*b*) O. M. Yaghi, H. Li, C. Davis, D. Richardson and T. L. Groy, *Acc. Chem. Res.*, 1998, **31**, 474; (*c*) O. R. Evans and W. Lin, *Acc. Chem. Res.*, 2002, **35**, 511; (*d*) M. J. Zaworotko, *Chem. Commun.*, 2001, 1; (*e*) P. J. Hagrman, D. Hagrman and J. Zubieta, *Angew. Chem., Int. Ed.*, 1999, **38**, 2638; (*f*) M. J. Zaworotko, *Chem. Soc. Rev.*, 1994, **23**, 283; (*g*) M. Eddaoudi, J. Kim, N. Rosi, D. Vodak, J. Wachter, M. O'Keeffe and O. M. Yaghi, *Science*, 2002, **295**, 469; (*h*) R. Robson, *J. Chem. Soc., Dalton Trans.*, 2000, 3735; (*i*) B. Moulton and M. J. Zaworotko, *Chem. Rev.*, 2001, **101**, 1629; (*j*) J. L. C. Rowsell and O. M. Yaghi, *Microporous Mesoporous Mater.*, 2004, **73**, 3.

2 (*a*) O. M. Yaghi, *Access in Nanoporous Materials*, ed. T. J. Pinnavaia and M. F. Thorpe, Plenum, New York, 1995, p. 111; (*b*) N. Guillou, S. Pastre, C. Livage and G. Ferey, *Chem. Commun.*, 2002, 2358; (*c*) B. Chen, M. Eddaoudi, S. T. Hyde, M. O'Keeffe and O. M. Yaghi, *Science*, 2001, **291**, 1021; (*d*) N. L. Rosi, J. Eckert, M. Eddaoudi, D. T. Vodak, J. Kim, M. O'Keeffe and O. M. Yaghi, *Science*, 2003, **300**, 1127; (*e*) J. S. Seo, D. Whang, H. Lee, S. I. Jun, J. Oh, Y. J. Jeon and K. Kim, *Nature*, 2000, **404**, 982; (*f*) O. Kahn and C. Martinez, *Science*, 1998, **279**, 44; (*g*) J. L. C. Rowsell, A. R. Millward, K. S. Park and O. M. Yaghi, *J. Am. Chem. Soc.*, 2004, **126**, 5666; (*h*) W. Lin, O. R. Evans, R. Xiong and Z. Wang, *J. Am. Chem. Soc.*, 1998, **120**, 13272; (*i*) B. Chen, N. W. Ockwig, A. R. Millward, D. S. Contreras and O. M. Yaghi, *Angew. Chem., Int. Ed.*, 2005, **44**, 4745.

3 N. Stock and S. Biswas, *Chem. Rev.*, 2012, **112**, 933.

4 (*a*) H.-K. Liu, T.-H. Tsao, Y.-T. Zhang and C.-H. Lin, *CrystEngComm*, 2009, **11**, 1462; (*b*) X.-F. Wang, Y.-B. Zhang, H. Huang, J.-P. Zhang and X.-M. Chen, *Cryst. Growth Des.*, 2008, **8**, 4559; (*c*) Y.-K. Seo, G. Hundal, I. T. Jang, Y. K. Hwang, C.-H. Jun and J.-S. Chang, *Microporous Mesoporous Mater.*, 2009, **119**, 331.

5 (*a*) S. R. Batten and R. Robson, *Angew. Chem., Int. Ed.*, 1998, **37**, 1460; (*b*) J. Kim, B. L. Chen, T. M. Reineke, H. L. Li, M. Eddaoudi, D. B. Moler, M. O'Keeffe and O. M. Yaghi, *J. Am. Chem. Soc.*, 2001, **123**, 8239; (*c*) S. M. Chen, C. Z. Lu, Q. Z. Zhang, J. H. Liu and X. Y. Wu, *Eur. J. Inorg. Chem.*, 2005, 423; (*d*) P. M. Forster, N. Stock and A. K. Cheetham, *Angew. Chem., Int. Ed.*, 2005, **44**, 7608.

6 (*a*) V. S. S. Kumar, F. C. Pigge and N. P. Rath, *New J. Chem.*, 2004, **28**, 1192; (*b*) A. J. Blake, N. R. Brooks, N. R. Champness, M. Crew, A. Deveson, D. Fenske, D. H. Gregory, L. R. Hanton, P. Hubberstey and M. Schroder, *Chem. Commun.*, 2001, 1432; (*c*) Y. J. Qi, Y. H. Wang, C. W. Hu, M. H. Cao, L. Mao and E. B. Wang, *Inorg. Chem.*, 2003, **42**, 8519.

7 (*a*) S.-Q. Zang, Y. Su, Y.-Z. Li, H.-Z. Zhu and Q.-J. Meng, *Inorg. Chem.*, 2006, **45**, 2972; (*b*) L. Pan, M. B. Sander, X.-Y. Huang, J. Li, M. Smith, E. Bittner, B. Bockrath and J. K. Johnson, *J. Am. Chem. Soc.*, 2004, **126**, 1308; (*c*) X.-L. Wang, C. Qin, E.-B. Wang, Y.-G. Li and Z.-M. Su, *Chem. Commun.*, 2005, 5450; (*d*) X.-L. Wang, C. Qin, E.-B. Wang, Y.-G. Li, Z.-M. Su, L. Xu and L. Carlucci, *Angew. Chem., Int. Ed.*, 2005, **44**, 5824; (*e*) X. L. Wang, C. Qin, E.-B. Wang and Z.-M. Su, *Chem. – Eur. J.*, 2006, **12**, 2680; (*f*) A. M. Plonka, D. Banerjee, W. R. Woerner, Z. Zhang, J. Li and J. B. Parise, *Chem. Commun.*, 2013, **49**, 7055; (*g*) T. Kundu, S. C. Sahoo and R. Banerjee, *Chem. Commun.*, 2012, **48**, 4998; (*h*) D. Banerjee, Z. Zhang, A. M. Plonka, J. Li and J. B. Parise, *Cryst. Growth Des.*, 2012, **12**, 2162; (*i*) A. M. Plonka, D. Banerjee, W. R. Woerner, Z. Zhang, N. Nijem, Y. J. Chabal, J. Li and J. B. Parise, *Angew. Chem., Int. Ed.*, 2013, **52**, 1692.

8 (*a*) C. T. Yeh, W. C. Lin, S. H. Lo, C. C. Kao, C.-H. Lin and C. C. Yang, *CrystEngComm*, 2012, **14**, 1219; (*b*) P.-C. Cheng, F.-S. Tseng, C.-T. Yeh, T.-G. Chang, C.-C. Kao, C.-H. Lin, W.-R. Liu, J.-S. Chen and V. Zima, *CrystEngComm*, 2012, **14**, 6812; (*c*) D. Senthil Raja, J.-H. Luo, C.-Y. Wu, Y.-J. Cheng, C.-T. Yeh, Y.-T. Chen, S.-H. Lo, Y.-L. Lai and C.-H. Lin, *Cryst. Growth Des.*, 2013, **13**, 3785.

9 (*a*) S. Noro, R. Kitaura, M. Kondo, S. Kitagawa, T. Ishii, H. Matsuzaka and M. Yamashita, *J. Am. Chem. Soc.*, 2002, **124**, 2568; (*b*) A. Kondo, H. Noguchi, L. Carlucci, D. M. Proserpio, G. Ciani, H. Kajiro, T. Ohba, H. Kanoh and K. Kaneko, *J. Am. Chem. Soc.*, 2007, **129**, 12362; (*c*) P. Pachfule, R. Das, P. Poddar and R. Banerjee, *Inorg. Chem.*, 2011, **50**, 3855; (*d*) J. Zhang, A. V. Biradar, S. Pramanik, T. J. Emge, T. Asefa and J. Li, *Chem. Commun.*, 2012, **48**, 6541; (*e*) S. Noro, Y. Hijikata, M. Inukai, T. Fukushima, S. Horike, M. Higuchi, S. Kitagawa, T. Akutagawa and T. Nakamura, *Inorg. Chem.*, 2013, **52**, 280.

10 (*a*) O. Khan, *Molecular Magnetism*, VCH, Weinheim, 1993; (*b*) R. L. Carlin, *Magnetochemistry*, Springer-Verlag, Berlin, Heidelberg, 1986.

11 (*a*) S. L. James, *Chem. Soc. Rev.*, 2003, **32**, 276; (*b*) H. C. Zhou, J. R. Long and O. M. Yaghi, *Chem. Rev.*, 2012, **112**, 673; (*c*) Y. Li, Z. Ju, B. Wu and D. Yuan, *Cryst. Growth Des.*, 2013, **13**, 4125.

12 (*a*) S. Shackley, D. Reiner, P. Upham, H. de Coninck, G. Sigurthorsson and J. Anderson, *Int. J. Greenhouse Gas Control*, 2009, **3**, 344; (*b*) J. F. M. Orr, *Energy Environ. Sci.*, 2009, **2**, 449.

13 W. Zhuang, H. Sun, H. Xu, Z. Wang, S. Gao and L. Jin, *Chem. Commun.*, 2010, **46**, 4339.

14 C.-Y. Li, J.-K. Su, C.-J. Yu, Y.-E. Tai, C.-H. Lin and B.-T. Ko, *Inorg. Chem. Commun.*, 2012, **20**, 60.

15 (*a*) *Bruker AXS, APEX2, V2010.3*, Bruker AXS Inc., Madison, WI; (*b*) *SADABS V2008/1; SAINT+ V7.60A*, Bruker AXS Inc., Madison, WI.

16 (*a*) *SHELXTL V6.14*, Bruker AXS Inc., Madison, WI, 2008; (*b*) G. M. Sheldrick, *Acta Crystallogr., Sect. A: Found. Crystallogr.*, 2008, **64**, 112.

17 A. C. Larson and R. B. Von Dreele, *General Structure Analysis System (GSAS)*, Los Alamos National Laboratory Report LAUR, 2000, 86–748.

18 T. Loiseaua, H. Muguerra, G. Férey, M. Haouas and F. Taulelle, *J. Solid State Chem.*, 2005, **178**, 621.

19 A. L. Spek, *J. Appl. Crystallogr.*, 2003, **36**, 7.

20 P. K. Thallapally, J. Tian, M. R. Kishan, C. A. Fernandez, S. J. Dalgarno, P. B. McGrail, J. E. Warren and J. L. Atwood, *J. Am. Chem. Soc.*, 2008, **130**, 16842.

21 Z. X. Zhao, Z. Li and Y. S. Lin, *Ind. Eng. Chem. Res.*, 2009, **48**, 10015.

22 J. Y. Lee, J. Li and J. Jagiello, *J. Solid State Chem.*, 2005, **178**, 2527.

23 S. Ma, X.-S. Wang, C. D. Collier, E. S. Manis and H.-C. Zhou, *Inorg. Chem.*, 2007, **46**, 8499.

24 H. R. Moon, N. Kobayashi and M. P. Suh, *Inorg. Chem.*, 2006, **45**, 8672.

25 A. M. Shultz, O. K. Farha, J. T. Hupp and S. T. Nguyen, *J. Am. Chem. Soc.*, 2009, **131**, 4204.

26 (*a*) H. J. Park and M. P. Suh, *Chem. Commun.*, 2010, 610; (*b*) S. Couck, J. M. Denayer, G. V. Baron, T. Remy, J. Gascon and F. Kapteijin, *J. Am. Chem. Soc.*, 2009, **131**, 6326; (*c*) X.-R. Meng, D.-C. Zhong, L. Jiang, H.-Y. Li and T.-B. Lu, *Cryst. Growth Des.*, 2011, **11**, 2020; (*d*) L. Bastin, P. S. Brcia, E. J. Hurtado, J. C. Silva, A. E. Rodrigues and B. Chen, *J. Phys. Chem. C*, 2008, **112**, 1575.

27 H. S. Choi and M. P. Suh, *Angew. Chem., Int. Ed.*, 2009, **48**, 6865.

28 C. J. Chuck, M. G. Davidson, M. D. Jones, G. Kociok-Kohn, M. D. Lunn and S. Wu, *Inorg. Chem.*, 2006, **45**, 6595.